POLARIMETRIC CLUTTER MODELING: THEORY AND APPLICATION

J. A. Kong, F. C. Lin, M. Borgeaud, H. A. Yueh, A. A. Swartz, and H. H. Lim

Department of Electrical Engineering and Computer Science
and Research Laboratory of Electronics
Massachusetts Institute of Technology
Cambridge, Massachusetts 02139

R. T. Shin and L. M. Novak

MIT Lincoln Laboratory
Lexington, MA 02173

ABSTRACT

The two-layer anisotropic random medium model is used to investigate fully polarimetric scattering properties of earth terrain media. The polarization covariance matrices for the untilted and tilted uniaxial random medium are evaluated using the strong fluctuation theory and distorted Born approximation. In order to account for the azimuthal randomness in the growth direction of leaves in tree and grass fields, an averaging scheme over the azimuthal direction is also applied. It is found that characteristics of terrain clutter can be identified through the analysis of each element of the covariance matrix. Theoretical results are illustrated by the comparison with experimental data provided by MIT Lincoln Laboratory for tree and grass fields.

I. INTRODUCTION

The layered random medium model for terrain cover, in conjunction with the application of electromagnetic wave theory, provides a systematic approach in relating the radar backscatter response to physical properties of geophysical media, where the volume scattering and anisotropic effects are attributed to the embedded inhomogeneities with elongated geometry and preferred alignment. For active and passive microwave remote sensing, the effectiveness of this model has been demonstrated by extraction of physical parameters from data matching for scene interpretation and feature identification [Zuniga *et al.*, 1980; Tsang and Kong, 1981; Tsang *et al.*, 1982; Lee and Kong, 1985; Lin *et al.*, 1988a, b]. In polarimetric microwave remote sensing, the random medium model has also been applied to radar image simulation, terrain clutter identification and classification, and radar range profile simulation of terrain clutter [Shin *et al.*, 1986; Borgeaud *et al.*, 1987a; Borgeaud, 1987b; Kong *et al.*, 1988; Yueh *et al.*, 1988a; Swartz *et al.*, 1988].

The theoretical modeling of earth terrain media is described in Section II. To account for the large permittivity contrast between the background medium and the embedded inhomogeneities, the strong fluctuation theory is applied in Section III, in order to derive the external field which is decomposed into mean (coherent part) and scattered field (incoherent part) components. The mean field is derived using the Feynman diagrammatic technique and bilocal approximation. In Section IV, the effective permittivity tensor of the medium is obtained from the constitutive relation. The effective permittivity tensor is computed in the low frequency limit for an unbounded uniaxial random medium with two-phase mixture. The distorted Born approximation is then used to calculate the scattered field in Section V. The polarization covariance matrices for the untilted and tilted uniaxial random medium, as well as that obtained from the azimuthal averaging of the tilted case are discussed in Section VI. Theoretical calculations of the fully polarimetric random medium model are compared with the experimental data for trees and a grass field supplied by MIT Lincoln Laboratory.

II. TWO-LAYER ANISOTROPIC RANDOM MEDIUM MODEL

The two-layer anisotropic random medium model is applied to simulate earth terrain media such as tree canopy and a grass field. In region 1 of Figure 1, the random medium with height d is characterized by a spatially random permittivity tensor $\bar{\bar{\epsilon}}_1(\bar{r})$. Regions 0 and 2 (air and ground) are considered to be homogeneous media with permittivities ϵ_0 and ϵ_2, respectively. All three regions are assumed to have the same permeability, μ_0. The polarimetric radar system is located in region 0. The coordinate system (x, y, z) is

oriented so that the xy plane coincides with the air/clutter interface. Interfaces at $z = 0$ and $z = -d$ are assumed to be planar, extending to infinity on the horizontal plane, and parallel to each other. The volume scattering effect is caused by randomly distributed scatterers embedded in the layer (e.g., moisture content in leaves) while the anisotropic effect is due to the elongated shape and preferred alignment of the scatterers. As shown in Figure 2, the moisture content in trees and grass is modeled as cylindrical scatterers with the preferred alignment in the yz plane. The elongated direction is along the z'-axis and tilted by an angle ψ with respect to the z-axis. Hence, the coordinate system (x', y', z') which describes the orientation of the scatterers is rotated clockwise by an angle ψ about the x-axis. In this manner, the z'-axis can be chosen as the optic axis of the permittivity tensor $\bar{\bar{\epsilon}}_1(\bar{r})$ [Kong, 1986].

In the polarimetric microwave remote sensing of terrain cover, the polarization covariance matrix is essential for terrain-feature identification and classification [Borgeaud *et al.*, 1987a; Kong *et al.*, 1988]. For a plane wave impinging on the random medium layer, the scattered electric field $\bar{E}_0^s(\bar{r})$ is related to the incident electric field $\bar{E}_{0i}(\bar{r})$ by

$$\begin{bmatrix} E_{hs} \\ E_{vs} \end{bmatrix} = \frac{e^{ikr}}{r} \begin{bmatrix} f_{hh} & f_{hv} \\ f_{vh} & f_{vv} \end{bmatrix} \begin{bmatrix} E_{hi} \\ E_{vi} \end{bmatrix} \tag{1}$$

where the horizontal and vertical components of the the incident and scattered electric fields are expressed as E_{hi}, E_{hs}, E_{vi}, and E_{vs}, respectively. For reciprocal media, the relation, $f_{vh} = f_{hv}$, is obtained in the backscattering direction. Thus, the covariance matrix is defined as

$$\bar{\bar{C}} \equiv \lim_{A \to \infty} \frac{4\pi}{A} \begin{bmatrix} \langle |f_{hh}|^2 \rangle & \langle f_{hh} f_{hv}^* \rangle & \langle f_{hh} f_{vv}^* \rangle \\ \langle f_{hv} f_{hh}^* \rangle & \langle |f_{hv}|^2 \rangle & \langle f_{hv} f_{vv}^* \rangle \\ \langle f_{vv} f_{hh}^* \rangle & \langle f_{vv} f_{hv}^* \rangle & \langle |f_{vv}|^2 \rangle \end{bmatrix} \tag{2}$$

where A is the illuminated area and $\langle X \rangle$ denotes the ensemble average of the random variable X. The covariance matrix is normalized so that the diagonal terms represent the backscattering cross sections per unit area for the HH, HV, and VV polarizations, respectively.

III. STRONG FLUCTUATION THEORY

Consider a linearly polarized time-harmonic electromagnetic plane wave impinging on the random medium. The time-harmonic factor $e^{-i\omega t}$ is used. The propagation vector $\overline{\kappa}_{0i}$ at the observation point has the incident angle θ_{0i} with respect to the z-axis (Fig. 1) and the azimuthal angle ϕ_{0i}. The total electric fields in regions 0 and 1 satisfy the following vector wave equations:

$$\nabla \times \nabla \times \overline{E}_0(\overline{r}) - k_0^2 \overline{E}_0(\overline{r}) = 0 \tag{3}$$

$$\nabla \times \nabla \times \overline{E}_1(\overline{r}) - k_0^2 \frac{\overline{\overline{\epsilon}}_1(\overline{r})}{\epsilon_0} \cdot \overline{E}_1(\overline{r}) = 0 \tag{4}$$

where $k_0^2 = \omega^2 \mu_0 \epsilon_0$. In the microwave frequency range, the dielectric constants of air and moisture content are very distinct. In order to account for the large permittivity contrast between the host medium and embedded inhomogeneities, a deterministic quantity $\overline{\overline{\epsilon}}_{g1}$ is introduced in the strong fluctuation theory [Ryzhov and Tamoikin, 1970; Tsang and Kong, 1981; Tsang *et al.*, 1982; Lin *et al.*, 1988a, b]. Equation (4) can then be rewritten as

$$\nabla \times \nabla \times \overline{E}_1(\overline{r}) - k_0^2 \frac{\overline{\overline{\epsilon}}_{g1}}{\epsilon_0} \cdot \overline{E}_1(\overline{r}) = k_0^2 \left(\frac{\overline{\overline{\epsilon}}_1(\overline{r}) - \overline{\overline{\epsilon}}_{g1}}{\epsilon_0} \right) \cdot \overline{E}_1(\overline{r})$$

$$\equiv k_0^2 \overline{\overline{Q}}_1(\overline{r}) \cdot \overline{E}_1(\overline{r}) \tag{5}$$

Physically, $\overline{\overline{\epsilon}}_{g1}$ is the effective permittivity tensor of the medium in the low frequency range where the scattering loss is negligible because the size of scatterers is much smaller than the wavelength of the incident field [Tsang *et al.*, 1985]. Treating the term on the right-hand side of (5) as the effective source, the total electric fields in regions 0 and 1 can be represented in integral forms as follows:

$$\overline{E}_0(\overline{r}) = \overline{E}_0^{(o)}(\overline{r}) + k_0^2 \int_{V_1} d^3\overline{r}_1 \overline{\overline{G}}_{01}(\overline{r}, \overline{r}_1) \cdot \overline{\overline{Q}}_1(\overline{r}_1) \cdot \overline{E}_1(\overline{r}_1) \tag{6}$$

$$\overline{E}_1(\overline{r}) = \overline{E}_1^{(o)}(\overline{r}) + k_0^2 \int_{V_1} d^3\overline{r}_1 \overline{\overline{G}}_{11}(\overline{r}, \overline{r}_1) \cdot \overline{\overline{Q}}_1(\overline{r}_1) \cdot \overline{E}_1(\overline{r}_1) \tag{7}$$

where the unperturbed electric fields, $\overline{E}_0^{(o)}(\overline{r})$ and $\overline{E}_1^{(o)}(\overline{r})$, are solutions to the homogeneous vector wave equations in (3) and (5) in the absence of the effective source term and the subscript V_1 denotes the volume of region 1. The dyadic Green's functions, $\overline{\overline{G}}_{01}(\overline{r}, \overline{r}_1)$ and $\overline{\overline{G}}_{11}(\overline{r}, \overline{r}_1)$, which correspond to the responses at $\overline{r}$ in regions 0 and 1, respectively,

due to a point source at $\bar{r}_1$ in the anisotropic homogeneous medium with the permittivity tensor $\bar{\bar{\epsilon}}_{s1}$, are governed by the following vector wave equations:

$$\nabla \times \nabla \times \bar{\bar{G}}_{01}(\bar{r}, \bar{r}_1) - k_0^2 \bar{\bar{G}}_{01}(\bar{r}, \bar{r}_1) = 0 \tag{8}$$

$$\nabla \times \nabla \times \bar{\bar{G}}_{11}(\bar{r}, \bar{r}_1) - k_0^2 \frac{\bar{\bar{\epsilon}}_{s1}}{\epsilon_0} \cdot \bar{\bar{G}}_{11}(\bar{r}, \bar{r}_1) = \bar{\bar{I}} \delta(\bar{r}, \bar{r}_1) \tag{9}$$

When the source and the observation points are in the same region, there is a singularity in the dyadic Green's function, which can be dealt with by separating $\bar{\bar{G}}_{11}(\bar{r}, \bar{r}_1)$ into principal value $PS\bar{\bar{G}}_{11}(\bar{r}, \bar{r}_1)$ and singular components, namely,

$$\bar{\bar{G}}_{11}(\bar{r}, \bar{r}_1) = PS\bar{\bar{G}}_{11}(\bar{r}, \bar{r}_1) - \frac{\bar{\bar{S}}_1}{k_0^2} \delta(\bar{r} - \bar{r}_1) \tag{10}$$

Thus, substituting (10) into (7) yields

$$\bar{F}_1(\bar{r}) = \bar{E}_1^{(o)}(\bar{r}) + k_0^2 \int_{V_1} d^3\bar{r}_1 PS\bar{\bar{G}}_{11}(\bar{r}, \bar{r}_1) \cdot \bar{\bar{\xi}}_1(\bar{r}_1) \cdot \bar{F}_1(\bar{r}_1) \tag{11}$$

$$\bar{F}_1(\bar{r}) \equiv \left[\bar{\bar{I}} + \bar{\bar{S}}_1 \cdot \bar{\bar{Q}}_1(\bar{r})\right] \cdot \bar{E}_1(\bar{r}) \tag{12}$$

$$\bar{\bar{\xi}}_1(\bar{r}) \equiv \bar{\bar{Q}}_1(\bar{r}) \cdot \left[\bar{\bar{I}} + \bar{\bar{S}}_1 \cdot \bar{\bar{Q}}_1(\bar{r})\right]^{-1} \tag{13}$$

Physically, $\bar{F}_1(\bar{r})$ can be interpreted as the external field [Ryzhov and Tamoikin, 1970].

The external field can be decomposed into a coherent part (mean field) $\left\langle \bar{F}_1(\bar{r}) \right\rangle$ and an incoherent part $\bar{\mathcal{F}}_1(\bar{r})$ (scattered field) [Tsang *et al.*, 1985]. Under the bilocal approximation, the mean field $\left\langle \bar{F}_1(\bar{r}) \right\rangle$ can be expressed as

$$\left\langle \bar{F}_1(\bar{r}) \right\rangle = \bar{E}_1^{(o)}(\bar{r}) + k_0^2 \int_{V_2} \int_{V_1} d^3\bar{r}_1 d^3\bar{r}_2 PS\bar{\bar{G}}_{11}(\bar{r}, \bar{r}_1) \cdot \bar{\bar{\xi}}_{1eff}(\bar{r}_1, \bar{r}_2) \cdot \left\langle \bar{F}_1(\bar{r}_2) \right\rangle \tag{14}$$

where

$$\bar{\bar{\xi}}_{1eff}(\bar{r}_1, \bar{r}_2) = k_0^2 \left\langle \bar{\bar{\xi}}_1(\bar{r}_1) \cdot PS\bar{\bar{G}}_{11}(\bar{r}_1, \bar{r}_2) \cdot \bar{\bar{\xi}}_1(\bar{r}_2) \right\rangle \tag{15}$$

Using the index notation, (15) can be expressed as

$$\left[\bar{\bar{\xi}}_{1eff}(\bar{r}_1, \bar{r}_2)\right]_{ip} = k_0^2 \Gamma_{lmnp} R_\ell(\bar{r}_1, \bar{r}_2) \left[\bar{\bar{G}}_{11}(\bar{r}_1, \bar{r}_2)\right]_{mn} + \Gamma_{lmnp} S_{mn} \delta(\bar{r}_1 - \bar{r}_2) \tag{16}$$

where Equation (10) was used and $\left\langle \xi_{1lm}(\bar{r}_1)\xi_{1np}(\bar{r}_2)\right\rangle$ has been replaced with the product of the variance, Γ_{lmnp} $(l,m,n,p = x,y,z)$, and the normalized correlation function, $R_\xi(\bar{r}_1,\bar{r}_2)$. For a statistically homogeneous medium, the normalized correlation function is a function of the displacement between $\bar{r}_1$ and $\bar{r}_2$, i.e.,

$$R_\xi(\bar{r}_1,\bar{r}_2) = R_\xi(\bar{r}_1 - \bar{r}_2) \tag{17}$$

Notice that the intrinsic properties of the embedded inhomogeneities are directly related to the volume scattering mechanism through the normalized correlation function in (14).

IV. EFFECTIVE PERMITTIVITY

The effective permittivity tensor for the uniaxial random medium is derived in this section, following the usual approach where the effect of boundary layers is neglected [Tsang and Kong, 1981; Stogryn, 1984]. In an unbounded uniaxial medium, with a quasi-static effective permittivity tensor of the form

$$\bar{\bar{\epsilon}}_{g1} = \begin{bmatrix} \epsilon_g & 0 & 0 \\ 0 & \epsilon_g & 0 \\ 0 & 0 & \epsilon_{gz} \end{bmatrix} \tag{18}$$

the mean field satisfies the following vector wave equation

$$\nabla\times\nabla\times\left\langle \overline{F}_1(\bar{r})\right\rangle - k_0^2\frac{\bar{\bar{\epsilon}}_{g1}}{\epsilon_0}\cdot\left\langle \overline{F}_1(\bar{r})\right\rangle + k_0^2\int_{-\infty}^{\infty} d^3\bar{r}_1\bar{\bar{\xi}}_{1eff}(\bar{r},\bar{r}_1)\cdot\left\langle \overline{F}_1(\bar{r}_1)\right\rangle = 0 \tag{19}$$

The dispersion relation, obtained from (19), allows the effective permittivity tensor for the medium to be defined as

$$\bar{\bar{\epsilon}}_{1eff}(\bar{k}) \equiv \bar{\bar{\epsilon}}_{g1} + \epsilon_0\bar{\bar{\xi}}_{1eff}(\bar{k}) = \begin{bmatrix} \epsilon_1 & 0 & 0 \\ 0 & \epsilon_1 & 0 \\ 0 & 0 & \epsilon_{1z} \end{bmatrix} \tag{20}$$

where $\bar{\bar{\xi}}_{1eff}(\bar{k})$ is the Fourier transform of $\bar{\bar{\xi}}_{1eff}(\bar{r}_1 - \bar{r}_2)$ as given in (16). In the low frequency limit, $\bar{\bar{\xi}}_{1eff}(\bar{k})$ can be approximated by

$$\left[\bar{\bar{\xi}}_{1eff}(0)\right]_{lp} = k_0^2\Gamma_{lmnp}\int_{-\infty}^{\infty} d^3\bar{k}\Phi_\xi(\bar{k})\left[\overline{\overline{G}}_g(\bar{k})\right]_{mn} + \Gamma_{lmnp}S_{mn} \tag{21}$$

where $\Phi_\ell(\bar{k})$ is the Fourier transform of the normalized correlation function $R_\ell(\bar{r})$. The Fourier transform of the dyadic Green's function $\overline{\overline{G}}_g(\bar{r})$ is given as

$$\overline{\overline{G}}_g(\bar{k}) = \frac{1}{\left(k_\rho^2 + k_z^2 - k_0^2\epsilon_g\right)k_\rho^2}\begin{bmatrix} k_y^2 & -k_x k_y & 0 \\ -k_y k_x & k_x^2 & 0 \\ 0 & 0 & 0 \end{bmatrix}$$

$$-\frac{1}{k_0^2\epsilon_{gz}\left[k_z^2 + \frac{\epsilon_g}{\epsilon_{gz}}\left(k_\rho^2 - k_0^2\epsilon_{gz}\right)\right]}\begin{bmatrix} \frac{k_x^2\left(k_\rho^2 - k_0^2\epsilon_{gz}\right)}{k_\rho^2} & \frac{k_x k_y\left(k_\rho^2 - k_0^2\epsilon_{gz}\right)}{k_\rho^2} & k_x k_z \\ \frac{k_y k_x\left(k_\rho^2 - k_0^2\epsilon_{gz}\right)}{k_\rho^2} & \frac{k_y^2\left(k_\rho^2 - k_0^2\epsilon_{gz}\right)}{k_\rho^2} & k_y k_z \\ k_z k_x & k_z k_y & k_z^2 - k_0^2\epsilon_g \end{bmatrix} \tag{22}$$

in which $k_\rho^2 = k_x^2 + k_y^2$. Analytical expressions for $\overline{\overline{\xi}}_{1ijj}(0)$ and the diagonal tensor $\overline{\overline{S}}_1$ are shown in Appendix A. For a two-phase mixture consisting of a background medium and scatterers with permittivities ϵ_b and ϵ_s, respectively, $\overline{\overline{\epsilon}}_{g1}$ can be evaluated from the following criterion [Tsang and Kong, 1981]:

$$\left\langle \overline{\overline{\xi}}_1(\bar{r}) \right\rangle = 0 \tag{23}$$

From (13) and (23), we obtain

$$\frac{\epsilon_b - \epsilon_g}{\epsilon_0 + S(\epsilon_b - \epsilon_g)}(1 - f_s) + \frac{\epsilon_s - \epsilon_g}{\epsilon_0 + S(\epsilon_s - \epsilon_g)}f_s = 0 \tag{24}$$

$$\frac{\epsilon_b - \epsilon_{gz}}{\epsilon_0 + S_z(\epsilon_b - \epsilon_{gz})}(1 - f_s) + \frac{\epsilon_s - \epsilon_{gz}}{\epsilon_0 + S_z(\epsilon_s - \epsilon_{gz})}f_s = 0 \tag{25}$$

where f_s is the fractional volume of scatterers. Equations (24) and (25) are the anisotropic version of Polder and van Santen's mixing formula [Polder and van Santen, 1946].

V. DISTORTED BORN APPROXIMATION

In the strong fluctuation theory, the original random medium is replaced with an equivalent random medium which has the permittivity, $\overline{\overline{\epsilon}}_{g1}$. This can be accomplished

without altering the characteristic of the volume scattering effect because the effective source defined in (5) remains intact, that is,

$$k_0^2 \overline{\overline{Q}}_1(\bar{r}) \cdot \overline{E}_1(\bar{r}) = k_0^2 \overline{\overline{\xi}}_1(\bar{r}) \cdot \overline{F}_1(\bar{r}) \tag{26}$$

where (12) and (13) have been used. From (6), the total electric field in region 0 can be rewritten as

$$\overline{E}_0(\bar{r}) = \overline{E}_0^{(o)}(\bar{r}) + k_0^2 \int_{V_1} d^3\bar{r}_1 \overline{\overline{G}}_{01}(\bar{r}, \bar{r}_1) \cdot \overline{\overline{\xi}}_1(\bar{r}_1) \cdot \overline{F}_1(\bar{r}_1)$$

$$\equiv \overline{E}_0^{(o)}(\bar{r}) + \overline{E}_0^{s}(\bar{r}) \tag{27}$$

where $\overline{E}_0^{s}(\bar{r})$ is the scattered electric field due to the effective source. By adopting the concept of the distorted Born approximation in quantum mechanics [Newton, 1966; Schiff, 1968], the scatterers are assumed to be embedded in the equivalent medium with the effective permittivity, $\overline{\overline{\epsilon}}_{1eff}(0)$ [Lang, 1981], so that the mean field, $\left\langle \overline{F}_1(\bar{r}) \right\rangle$, is used to approximate the external field, $\overline{F}_1(\bar{r})$, and the mean dyadic Green's function, $\left\langle \overline{\overline{G}}_{01}(\bar{r}, \bar{r}_1) \right\rangle$, is used to replace $\overline{\overline{G}}_{01}(\bar{r}, \bar{r}_1)$. The following vector wave equations:

$$\nabla \times \nabla \times \left\langle \overline{F}_1(\bar{r}) \right\rangle - k_0^2 \frac{\overline{\overline{\epsilon}}_{1eff}(0)}{\epsilon_0} \cdot \left\langle \overline{F}_1(\bar{r}) \right\rangle = 0 \tag{28}$$

$$\nabla \times \nabla \times \left\langle \overline{\overline{G}}_{10}(\bar{r}, \bar{r}_1) \right\rangle - k_0^2 \frac{\overline{\overline{\epsilon}}_{1eff}(0)}{\epsilon_0} \cdot \left\langle \overline{\overline{G}}_{10}(\bar{r}, \bar{r}_1) \right\rangle = 0 \tag{29}$$

in conjunction with the symmetric property of the dyadic Green's functions, namely, $\left\langle \overline{\overline{G}}_{01}(\bar{r}, \bar{r}_1) \right\rangle = \left\langle \overline{\overline{G}}_{10}(\bar{r}_1, \bar{r}) \right\rangle^T$, are used to derive the mean field and the mean dyadic Green's function for the scattered electric field which can be written as

$$\overline{E}_0^{s}(\bar{r}) = k_0^2 \int_{V_1} d^3\bar{r}_1 \left\langle \overline{\overline{G}}_{01}(\bar{r}, \bar{r}_1) \right\rangle \cdot \overline{\overline{\xi}}_1(\bar{r}_1) \cdot \left\langle \overline{F}_1(\bar{r}_1) \right\rangle \tag{30}$$

Physically, the scattered electric field, under the distorted Born approximation, corresponds to the single scattering of the coherent fields [Tsang, *et al.*, 1985]. It is also known as the first-order multiple scattering [Ishimaru, 1978]. After decomposing $\overline{E}_0^{s}(\bar{r})$ into horizontal and vertical components and making use of (1) and (2), the nine elements of the polarization covariance matrix can be computed.

VI. DATA MATCHING AND APPLICATIONS

Data Matching

For an untilted uniaxial random medium, the optic axis is in the z-direction, $\psi = \psi_f = 0$. For vertically and horizontally polarized incident fields, the single scattering process in the distorted Born approximation does not depolarize the incident field in the backscattering direction and the coefficient f_{hv} vanishes. Hence, the covariance matrix becomes

$$\overline{\overline{C}} = \sigma \begin{bmatrix} 1 & 0 & \rho\sqrt{\gamma} \\ 0 & 0 & 0 \\ \rho^*\sqrt{\gamma} & 0 & \gamma \end{bmatrix} \tag{31}$$

where σ is the backscattering coefficient for the HH polarization, γ is the copolarization intensity ratio $(\sigma_{vv}/\sigma_{hh})$, and ρ is the normalized correlation coefficient between HH and VV returns given by

$$\rho \equiv \frac{\langle f_{hh} f_{vv}^* \rangle}{\sigma\sqrt{\gamma}} \tag{31b}$$

In general, for the case of tilted uniaxial random medium $(\psi = \psi_f \neq 0)$, depolarization effects exist even in the single scattering process, and the nine elements of the covariance matrix are all nonzero, i.e.,

$$\overline{\overline{C}} = \sigma \begin{bmatrix} 1 & \beta\sqrt{e} & \rho\sqrt{\gamma} \\ \beta^*\sqrt{e} & e & \xi\sqrt{\gamma e} \\ \rho^*\sqrt{\gamma} & \xi^*\sqrt{\gamma e} & \gamma \end{bmatrix} \tag{32}$$

where

$$\beta \equiv \frac{\langle f_{hh} f_{hv}^* \rangle}{\sigma\sqrt{e}} \tag{32a}$$

$$\xi \equiv \frac{\langle f_{hv} f_{vv}^* \rangle}{\sigma\sqrt{e\gamma}} \tag{32b}$$

are the correlation coefficients between the HH and HV and HV and VV channels, respectively. However, when the downward propagation vector $\overline{\kappa}_{0i}$ lies in the yz plane, i.e., $\phi_{0i} = 90°$, both the double refraction phenomenon and the depolarization effect in the

backscattering direction disappear so that $f_{hv} = 0$ [Lee and Kong, 1985a]. Under this condition, the covariance matrix also retains the same form as the untilted case, as shown in (31). It should be noted that the growth directions of leaves in trees and grass fields are not necessarily aligned in one direction. In order to account for the random orientation of the scatterers in the azimuthal direction, an azimuthal averaging scheme [Borgeaud, 1987b] is applied to derive the polarization covariance matrix. It is found that although $f_{hv} \neq 0$, four of the elements in the covariance matrix reduce to zero [Borgeaud *et al.*, 1987a; Kong *et al.*, 1988]. Thus the polarization covariance matrix becomes

$$\overline{\overline{C}} = \sigma \begin{bmatrix} 1 & 0 & \rho\sqrt{\gamma} \\ 0 & e & 0 \\ \rho^*\sqrt{\gamma} & 0 & \gamma \end{bmatrix} \tag{33}$$

The existence of the four zero elements is due to the fact that the random medium possesses an azimuthal symmetry in a statistical sense. The four zero elements of the covariance matrix indicate that there is no correlation between the copolarization (HH and VV) and cross-polarization (HV) returns, i.e., $\beta = 0$ and $\xi = 0$.

In order to illustrate the random medium model, polarimetric data for forests and grass fields obtained from MIT Lincoln Laboratory are matched with this model. The operating frequency was 35 GHz, and the angle of incidence was 82°. Measured covariance matrices for grass and tree regions, given in Table 1, were calculated from the blocked out regions shown in Figure 7 of [Swartz *et al.*, 1988]. Analysis of this database indicated that there is essentially no correlation between the HH and HV, and between the HV and VV polarimetric returns; from a statistical point of view the terrain clutter exhibited azimuthal symmetry, and therefore $\beta \simeq 0$ and $\xi \simeq 0$. Thus, the form of the covariance matrix shown in (33) was utilized. The corresponding theoretically calculated covariance matrix parameters, also shown in Table 1, were obtained by azimuthal averaging [Borgeaud, 1987b] of the covariance matrices obtained using the two-layer anisotropic random medium model with the application of the strong fluctuation theory and distorted Born approximation.

Applications

The random medium model provides a systematic approach for the design of optimal target detection and classification algorithms [Novak *et al.*, 1987] and the identification of terrain media such as vegetation canopy, forest, and snow-covered fields using the optimum polarimetric classifier [Kong *et al.*, 1988]. The polarization covariance matrices for various

terrain covers were computed from theoretical models of random medium. The optimal classification scheme made use of a quadratic distance measure and was applied to classify a vegetation canopy consisting of both trees and grass; i.e., using the fully polarimetric covariance matrix for the scattered fields, the Bayes likelihood ratio test was performed on specific measurements to classify the terrain into different categories. The Bayes likelihood ratio test has been shown to be optimal in the sense that it minimizes the probability of error [Fukunaga, 1972; Hord, 1986; Richards, 1986; Swain, 1978].

The probabilities of error obtained using fully polarimetric data were compared with the probabilities of error obtained using several single, polarimetrically derived features. For each single feature studied, the corresponding probability density function was derived. Once the probability density functions were known, the Bayes likelihood ratio test was performed to classify terrain elements into different categories. For classification schemes based on single features, closed-form expressions for the probability of error were calculated [Kong *et al.*, 1988].

A supervised Bayes classification was applied to synthetic aperture radar (SAR) polarimetric images in order to identify their various earth terrain components [Lim *et al.*, 1988]. Both fully polarimetric and normalized polarimetric classifications were employed to classify radar imagery. It was again shown, in this case through use of radar images, that fully polarimetric classifications yielded optimal results; however, an optimal normalized classification scheme [Yueh *et al.*, 1988b] indicated improved performance in regions where the absolute backscattering coefficients differed significantly from that of the training regions due to the variation in return power as a function of incident angle.

The Bayes classification is known to give minimum probability of error as long as the statistical distributions of the radar returns are known and the training areas are accurate. However, as noted above, the selected training regions were not sufficient to classify correctly the entire image due to the variation in incident angle over the imaged swath. By employing the random medium model to generate the classifier training data, the effect of the incident angle can be included in the classification scheme.

Another application of the fully polarimetric, multi-incident angle and frequency random medium model is to match training data from various image regions, say at one frequency and during one particular season, and then generate classifier training data which will predict the backscattered response of the terrain at different frequencies and during different seasons of the year. For example, the effects of the winter season can be simulated by adding a layer of snow to a terrain from which training data was recorded

during the summer season. In this manner, data need not be collected for all seasons and at all frequencies. The random medium model can be used to predict the backscattered response based on the initial training data.

APPENDIX A

The normalized correlation function, $R_\xi(x', y', z')$, for the unbounded uniaxial random medium in the (x', y', z') coordinate frame is assumed to be

$$\exp\left[-\frac{|x'|}{l_\rho} - \frac{|y'|}{l_\rho} - \frac{|z'|}{l_z}\right] \tag{A1}$$

so that $\bar{\bar{\xi}}_{1eff}$ is given by

$$\bar{\bar{\xi}}_{1eff}(0) = \begin{bmatrix} \Gamma_{xxxx}(I+S) & 0 & 0 \\ 0 & \Gamma_{yyyy}(I+S) & 0 \\ 0 & 0 & \Gamma_{zzzz}(I_z+S_z) \end{bmatrix} \tag{A2}$$

where

$$\Gamma_{xxxx} = \Gamma_{yyyy} = \langle \xi^2(\bar{r}) \rangle \equiv \delta_\rho \tag{A3}$$

$$\Gamma_{zzzz} = \langle \xi_z^2(\bar{r}) \rangle \equiv \delta_z \tag{A4}$$

and

$$I = \frac{\epsilon_0 \zeta}{\pi \epsilon_s (\alpha+2)} \left\{ \frac{2}{\sqrt{\alpha+1}} \log\left[\frac{\left(\sqrt{\alpha-\zeta}+\sqrt{\alpha+1}\right)\left(\sqrt{\alpha+1}+1\right)}{\sqrt{\alpha-\zeta}-i\sqrt{\zeta(\alpha+1)}} \right] \right.$$

$$\left. - 2\sqrt{\frac{\alpha-\zeta}{\zeta+2}} \log\left[\frac{\sqrt{2}\left(\sqrt{\zeta+2}-1\right)}{\sqrt{\zeta+2}+i\sqrt{\zeta}} \right] - \frac{\pi}{2} \right\}$$

$$- \frac{\epsilon_0}{\pi \epsilon_s (\beta+2)} \left\{ \frac{2(\beta-\chi)}{\sqrt{\beta+1}} \log\left[\frac{\left(\sqrt{\beta-\chi}+\sqrt{\beta+1}\right)\left(\sqrt{\beta+1}+1\right)}{\sqrt{\beta-\chi}-i\sqrt{\chi(\beta+1)}} \right] \right.$$

$$\left. + 2\sqrt{(\beta-\chi)(\chi+2)} \log\left[\frac{\sqrt{2}\left(\sqrt{\chi+2}-1\right)}{\sqrt{\chi+2}+i\sqrt{\chi}} \right] + \frac{\pi(\chi+2)}{2} \right\} \tag{A5}$$

$$I_s = \frac{2\epsilon_0}{\pi\epsilon_{gs}(\beta+2)}\left\{\frac{2\beta}{\sqrt{\beta+1}}\log\left[\frac{\left(\sqrt{\beta-\chi}+\sqrt{\beta+1}\right)\left(\sqrt{\beta+1}+1\right)}{\sqrt{\beta-\chi}-i\sqrt{\chi(\beta+1)}}\right]\right.$$

$$\left. + 4\sqrt{\frac{\beta-\chi}{\chi+2}}\log\left[\frac{\sqrt{2}\left(\sqrt{\chi+2}-1\right)}{\sqrt{\chi+2}+i\sqrt{\chi}}\right] - \frac{\pi\beta}{2}\right\} \qquad (A6)$$

where

$$\zeta = \frac{\epsilon_g}{\epsilon_0}k_0^2 l_\rho^2, \qquad \chi = \frac{\epsilon_{gs}}{\epsilon_g}\zeta, \qquad \alpha = \zeta + \frac{l_\rho^2}{l_z^2}, \qquad \beta = \frac{\epsilon_{gs}}{\epsilon_g}\alpha \qquad (A7)$$

The components of $\overline{\overline{S}}_1$ are obtained from the frequency-independent part of (A5) and (A6):

$$S = \frac{\epsilon_0}{\epsilon_g(\eta^2+2)}\left\{\frac{2\eta^2}{\pi\sqrt{(\eta^2+1)}}\log\left[\frac{\eta\sqrt{\eta^2+1}+\eta^2}{\sqrt{\eta^2+1}-1}\right]\right.$$

$$\left. - \frac{\sqrt{2}\eta}{\pi}\log\left[\frac{\sqrt{2}+1}{\sqrt{2}-1}\right] + 1\right\} \qquad (A8)$$

$$S_z = -\frac{\epsilon_0}{\epsilon_{gz}(\eta^2+2)}\left\{\frac{4\eta^2}{\pi\sqrt{(\eta^2+1)}}\log\left[\frac{\eta\sqrt{\eta^2+1}+\eta^2}{\sqrt{\eta^2+1}-1}\right]\right.$$

$$\left. - \frac{2\sqrt{2}\eta}{\pi}\log\left[\frac{\sqrt{2}+1}{\sqrt{2}-1}\right] - \eta^2\right\} \qquad (A9)$$

$$\eta = \sqrt{\frac{\epsilon_{gz}l_\rho^2}{\epsilon_g l_z^2}} \qquad (A10)$$

From (A8) and (A9), it can be shown that S and S_z satisfy the condition [Stogryn, 1983]:

$$2\frac{\epsilon_g}{\epsilon_0}S + \frac{\epsilon_{gz}}{\epsilon_0}S_z = 1 \qquad (A11)$$

ACKNOWLEDGEMENTS

This work was supported by ARMY Corp of Engineers contract DACA39-87-K-0022, a SIMTECH contract, NASA Grant NAG5-270, and ONR contract N00014-83-K-0258.

This work was also sponsored by the Defense Advanced Research Projects Agency. The views expressed are those of the authors and do not reflect the official policy or position of the U.S. Government.

REFERENCES

Borgeaud, M., R. T. Shin, and J. A. Kong (1987a), "Theoretical models for polarimetric radar clutter," *J. of Electromagnetic Waves and Applications*, 1(1), pp. 67–86.

Borgeaud, M. (1987b), "*Theoretical Models for Polarimetric Microwave Remote Sensing of Earth Terrain*," Ph. D. Dissertation, Massachusetts Institute of Technology, Jan. 1988.

Fukunaga, K. (1972), **Introduction to Statistical Pattern Recognition**, Academic Press, New York.

Ishimaru, A. (1978), **Wave Propagation and Scattering in Random Media**, Vol. 1 and 2, Academic Press, New York.

Kong, J. A., A. A. Swartz, H. A. Yueh, L. M. Novak, and R. T. Shin (1988), "Identification of terrain cover using the optimum polarimetric classifier," *J. of Electromagnetic Waves and Applications*, 2(2), pp. 171–194.

Kong, J. A. (1986), **Electromagnetic Wave Theory**, Wiley-Interscience, New York.

Lang, R. H. (1981), "Electromagnetic backscattering from a sparse distribution of lossy dielectric scatterers," *Radio Science*, 16(1), pp. 15–30.

Lee, J. K. and J. A. Kong (1985), "Active microwave remote sensing of an anisotropic random medium layer," *IEEE Trans. Geosci. and Remote Sensing*, GE-23(6), pp. 910–923.

Lim, H. H., A. A. Swartz, H. A. Yueh, J. A. Kong, R. T. Shin, and J. J. van Zyl (1988), "Classification of earth terrain using polarimetric synthetic aperture radar imagery," URSI Meeting, Syracuse, NY, June 6 – 10.

Lin, F. C., J. A. Kong, R. T. Shin, A. J. Gow, and S. A. Arcone (1988a), "Correlation function study for sea ice," *J. Geophy. Res.*, accepted for publication.

Lin, F. C., J. A. Kong, R. T. Shin, A. J. Gow, and D. Perovich (1988b), "Theoretical model for snow-covered sea ice," *IEEE AP-S International Symposium & URSI Radio Science Meeting,* Syracuse University, Syracuse, New York, June 6–10.

ewton, R. G. (1966), **Scattering Theory of Waves and Particles,** McGraw-Hill Book Company, Inc., New York.

vak, L. M., M. B. Sechtin, and M. J. Cardullo (1987), "Studies of target detection algorithms that use polarimetric radar data," *IEEE Proceedings of the Nineteenth Asilomar Conference on Circuits, Systems, and Computers,* Pacific Grove, CA, Nov 1–3.

oulis, A. (1984), **Probability, Random Variables, and Stochastic Processes,** McGraw-Hill Book Company, New York.

ler, D. and J. H. van Santen (1946), "The effective permeability of mixtures of solids," *Physica,* 12(5), pp. 257-271.

ards, J. A. (1986), **Remote Sensing Digital Image Analysis,** Springer-Verlag, New York.

ov, Y. A. and V. V. Tamoikin (1970), "Radiation and propagation of electromagnetic vaves in randomly inhomogeneous media," *Radiophysics Quantum Electron.,* 13(3), p. 273–300.

, L. I. (1968), **Quantum Mechanics,** 3rd Ed., McGraw-Hill Book Company, Inc., ew York.

R. T., L. M. Novak, and M. Borgeaud (1986), "Theoretical models for polarimetric dar clutter," *Tenth DARPA/Tri-Service Millimeter Wave Symposium,* U.S. Army arry Diamond Laboratories, Adelphi, MD, April 8–10.

, A. (1984), "The bilocal approximation for the effective dielectric constant of an tropic random medium," *IEEE Trans. Ant. and Propag.,* AP-32(5), pp. 517–520.

, A. (1983), "A note on the singular part of the dyadic Green's function in strong fluctuation theory," *Radio Science,* 18(6), pp. 1283–1286.

Swain, P. H. and S. M. Davis (ed.) (1978), **Remote Sensing: The Quantitative Approach,** McGraw-Hill, New York.

Swartz, A. A., L. M. Novak, R. T. Shin, D. A. McPherson, A. V. Saylor, F. C. Lin, H. A. Yueh, and J. A. Kong (1988), "Radar range profile simulation of terrain clutter using the random medium model," in *GACIAC PR-88-03, The Polarimetric Technology Workshop,* Rocket Auditorium, Redstone Arsenal, U. S. Army Missile Command, Huntsville, Alabama, August 16–19.

Tai, C. T. (1971), **Dyadic Green's Functions in Electromagnetic Theory**, Intex Educational Publishers, Scranton, Pennsylvania.

Tsang, L., J. A. Kong, and R. T. Shin (1985), **Theory of Microwave Remote Sensing**, Wiley-Interscience, New York.

Tsang, L., J. A. Kong, and R. W. Newton (1982), "Application of strong fluctuation random medium theory to scattering of electromagnetic waves from a half-space of dielectric mixture," *IEEE Trans. Ant. and Propag.*, AP-30(2), pp. 292–302.

Tsang, L. and J. A. Kong (1981), "Application of strong fluctuation random medium theory to scattering from vegetation-like half space," *IEEE Trans. Geosci. and Remote Sensing,* GE-19(1), pp. 62–69.

Yueh, H. A., S. V. Nghiem, Lin, F. C., J. A. Kong, and R. T. Shin (1988a), "Three-layer random medium model for polarimetric remote sensing of earth terrain," *IEEE AP-S International Symposium & URSI Radio Science Meeting,* Syracuse University, Syracuse, New York, June 6–10.

Yueh, H. A., A. A. Swartz, J. A. Kong, R. T. Shin and L. M. Novak (1988b), "Optimal classification of terrain cover using normalized polarimetric data," *J. Geophy. Res.*, accepted for publication.

Zuniga, M., J. A. Kong, and L. Tsang (1980), "Depolarization effects on the active remote sensing of random media," *J. Appl. Phys.*, 51(5), pp. 2315–2325.

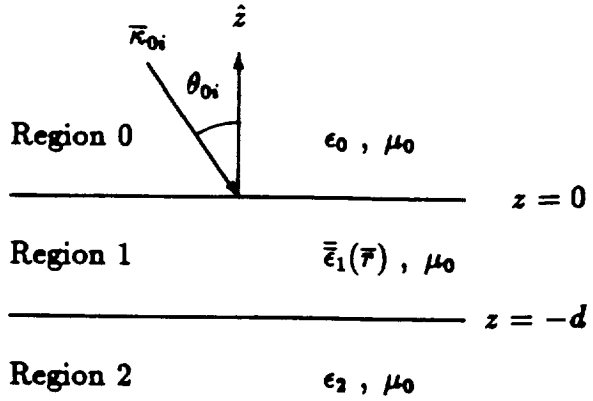

Figure 1 : Anisotropic two-layer random medium configuration.

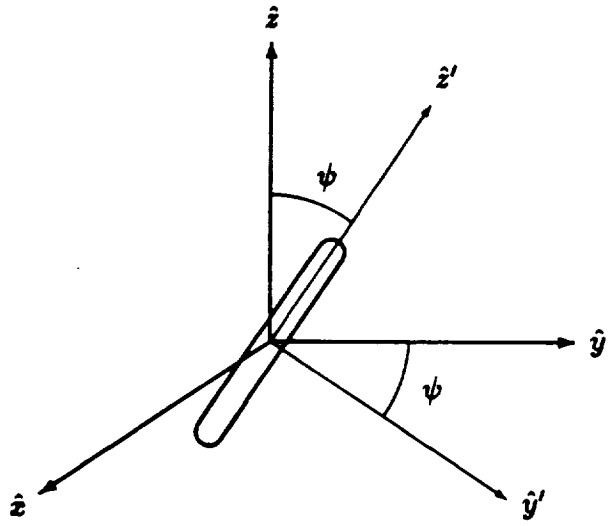

Figure 2 : Geometry of the permittivity tensor in the anisotropic random medium.

(a)

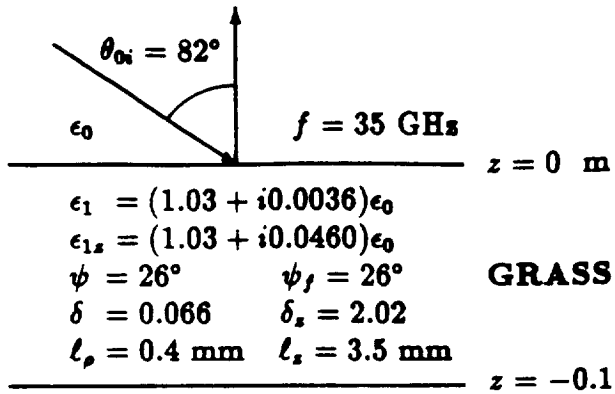

	σ (dB)	e	γ	$\lvert\rho\rvert$	ϕ_ρ
Experiment	−14.5	0.19	1.4	0.54	3.5°
Theory	−14.4	0.17	1.3	0.59	3.6°

(b)

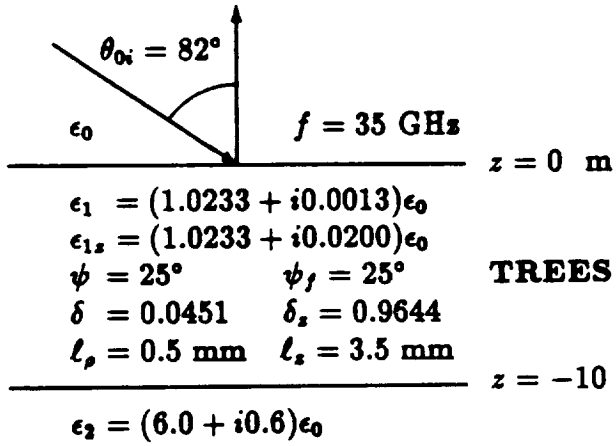

	σ (dB)	e	γ	$\lvert\rho\rvert$	ϕ_ρ
Experiment	−10.8	0.12	1.2	0.64	0.7°
Theory	−10.6	0.12	1.2	0.65	4.5°

Table 1 : Covariance matrix elements for grass (a) and trees (b).